A Model Investigation of Aerosol-Induced Changes in the East Asian Winter Monsoon

Liu Zhen (Orcid ID: 0000-0001-9197-0229)
Ming Yi (Orcid ID: 0000-0002-5324-1305)
Wang Lin (Orcid ID: 0000-0002-3557-1853)
Bollasina Massimo (Orcid ID: 0000-0001-7509-7650)
Yim Steve H.L. (Orcid ID: 0000-0002-2826-0950)

A Model Investigation of Aerosol-Induced Changes in the East Asian Winter Monsoon

Zhen Liu[1,2,3], Yi Ming[4], Lin Wang[5], Massimo Bollasina[3], Ming Luo[6,2], Ngar-Cheung Lau[2,7,1], Steve Hung-Lam Yim[7,2,1]

[1]Institute of Space and Earth Information Science, The Chinese University of Hong Kong, Hong Kong, China

[2]Institute of Environment, Energy and Sustainability, The Chinese University of Hong Kong, Sha Tin, N.T., Hong Kong

[3]School of Geosciences, University of Edinburgh, UK

[4]Geophysical Fluid Dynamics Laboratory/NOAA, Princeton, New Jersey, USA

[5]Center for Monsoon System Research, Institute of Atmospheric Physics, Chinese Academy of Science, Beijing, China

[6]School of Geography and Planning, and Guangdong Key Laboratory for Urbanization and Geo-simulation, Sun Yat-sen University, Guangzhou 510275, China

[7]Department of Geography and Resource Management, The Chinese University of Hong Kong, Sha Tin, N.T., Hong Kong

Corresponding author: Hung-Lam Steve Yim (steveyim@cuhk.edu.hk); Ngar-Cheung Lau (gabriel.lau@cuhk.edu.hk)

Key Points:

- Anthropogenic aerosols enhance the East Asian winter monsoon circulation north of 30˚N but weaken it south of 30˚N.
- The precipitation increases over South China is primarily associated with an anomalous anticyclone to the southwest of the Philippines.
- The tropical circulation changes are related to a southward shift of the local Hadley circulation driven by asymmetrical aerosol forcing.

This article has been accepted for publication and undergone full peer review but has not been through the copyediting, typesetting, pagination and proofreading process which may lead to differences between this version and the Version of Record. Please cite this article as doi: 10.1029/2019GL084228

Abstract

The response of the East Asian winter monsoon (EAWM) circulation to aerosols is studied using a coupled atmosphere-slab ocean general circulation model. In the extratropics, the aerosol-induced cooling in the mid-latitudes leads to an intensified subtropical jet stream, a deepened East Asian trough, and thus an enhanced EAWM. In the tropics, the local Hadley circulation shifts southward to compensate for the interhemispheric asymmetry in aerosol radiative cooling. Anomalous subsidence at around 10˚N leads to a salient anticyclone to the southwest of the Philippines. The associated southwesterlies advect abundant moisture to South China, resulting in local precipitation increase and suggesting a weaker EAWM. The EAWM response to aerosol forcing is thus driven by a competition between tropical and extratropical mechanisms, which has important implications for the future monsoon evolution as aerosol changes may follow different regional-dependent trajectories.

Plain Language Summary

In this study, we use a global atmospheric model to examine how aerosols affect the East Asian winter monsoon intensity, which modulates the strength of cold air outbreaks in East Asia. The aerosol-induced cooling mainly appears in the Northern Hemisphere mid-latitude land and their downwind ocean regions. The cooling enhances the East Asian winter monsoon north of 30˚N, with stronger northerly winds and colder winters there. However, aerosols weaken the East Asian winter monsoon south of 30˚N, with intensified southerly winds bringing warm and moist air to South China, thus resulting in enhanced precipitation. The larger magnitude of the southerly south of 30˚N than that of the northerly north of 30˚N and increased precipitation over South China suggest a considerable influence of aerosols on East Asian winter monsoon through tropical circulation changes.

1 Introduction

The Asian continent, home to 60% of world population, is affected by two serious environmental issues: air pollution and monsoon-induced floods and droughts (Lau et al., 2008). In recent decades, rapid urbanization and economic development have dramatically increased the anthropogenic aerosol loading in Asian countries. These changes pose severe threats to human health and the environment. Besides, aerosols may significantly alter the Earth energy budget through absorbing and scattering solar radiation (the direct effects) as well as by changing cloud microphysical processes (the indirect effects; e.g., Huang et al., 2014; Koren et al., 2014; Yeh et al., 2015, 2017; Kim et al., 2019). Both observational and modeling results have shown a strong impact of aerosols on monsoon circulation and precipitation over Asia (e.g., Ramanathan et al., 2001; Lau et al., 2006; Nakajima et al., 2007; Bollasina et al., 2011; Li et al., 2011). However, the majority of the studies focused on the summer (e.g., Guo et al., 2013; Bollasina et al., 2014; Das et al., 2014; Kim et al., 2016), while the possible influence of aerosols on the East Asian winter monsoon (EAWM) remain mostly unexplored.

The EAWM is a key component of the climate system over Asia. Its large meridional extent results in interactions with circulation in both the tropics and extra-tropics, such as the Siberian-Mongolian high, the mid-level East Asian trough centered along the longitudes of Japan, the upper-tropospheric jet stream over East Asia, and the near-equatorial convection (Wang et al., 2010). The EAWM climatological flow pattern is characterized by strong northwesterlies along the eastern flank of the Siberian high north of 30˚N (Lau and Chang, 1987; Ding, 1994) and northeasterlies along the East Asian coastline toward the South China Sea (SCS) south of 30˚N (Chen et al., 2000). The EAWM variability is modulated by tropical-extratropical interactions (Chang et al., 2006, 2011) and manifests latitudinal-dependent

characteristics (Wang et al., 2010; Liu et al., 2012; Chen et al., 2014). A stronger EAWM is characterized by an enhanced jet stream, a deepened East Asian trough, a stronger Siberian-Mongolian high and Aleutian low, and intensified northeasterly flow along the Russian coast (Jhun and Lee, 2004). During strong EAWM years, precipitation is enhanced over the Maritime Continent and reduced along the monsoonal front extending from southeastern China to the northwestern Pacific (Wang and Chen, 2014).

Given the above interactions of the EAWM with the large-scale circulation, it is conceivable that aerosol imprint on the EAWM may occur via changes in both the tropics and extra-tropics. On one hand, the midlatitude cooling due to increased aerosol enhances (weakens) the meridional temperature gradient equatorward (poleward) of the Northern Hemisphere (NH) subtropical jet (Ming et al., 2011, hereafter M11). This induces a southward movement of the jet stream, leading to a simultaneous intensification of the subtropical jet and a weakening of the polar front jet which, in turn, result in a stronger EAWM. On the other hand, the aerosols-induced cooling of the NH compared to the SH causes an interhemispheric energy imbalance. To reduce this asymmetry, the atmosphere circulation tends to transport energy in the meridional direction from the SH to the NH, manifested by a southward shift of the Hadley circulation (Ming and Ramaswamy, 2011; Hwang et al., 2013). Accompanied by the Hadley circulation shift, the changes in EAWM remain unclear even though which is closely related to tropical circulations (Chang et al., 2006).

These findings suggest the need to examine the EAWM variability, and in particular, its response to aerosol forcing accounting for its multifaceted links with tropical and extratropical circulation features (Liu et al., 2013) which may possibly result in diverse monsoon changes. Yet, to our knowledge, such a comprehensive assessment of the aerosol-driven changes to the EAWM has not been conducted so far. Jiang et al. (2017) noted that the aerosol-induced cooling in northern East Asia leads to an accelerated jet stream around 40˚N, thus contributing to an intensified EAWM over northern East Asia. However, they did not examine the aerosol-induced changes in tropical circulation and their effects on the EAWM circulation. In this study, we aim to fill the above gap by identifying both the tropical and extratropical circulation responses to aerosols and their influences on the EAWM by analyzing output of a general circulation model. The precipitation response over South China, where most precipitation occurs during winter (Figure S10a), is also discussed.

The model configuration and experiment design are described in Section 2. The aerosol-induced changes in the EAWM and precipitation are examined in Section 3, where the distinct tropical and extratropical responses are discussed. Finally, the main conclusions are summarized in Section 4.

2 Model Configuration and Experiment Design

To understand the influence of aerosols on the EAWM, we analyze a set of experiments using the Geophysical Fluid Dynamics Laboratory (GFDL) Atmospheric Model version 2.1 (AM2.1; GFDL Global Atmospheric Model Development 2004) coupled with a slab ocean model. The atmospheric component is configured with a latitude-longitude resolution of 2˚ × 2.5˚. Both the aerosol direct and indirect effects are considered with the latter parameterized by implementing a prognostic scheme of cloud droplet number concentration (Ming et al., 2007). The burdens of tropospheric aerosols and ozone are prescribed using monthly mean outputs from a chemical transport model (Horowitz, 2006). A comparison of the simulated aerosol concentration, optical depth, and cloud properties with observations shows that the model is able to capture their main spatial-temporal features (Ginoux el al., 2006; Ming et al., 2007). More information about aerosols is provided in the supplementary material (see Text

S1 and S3). Two experiments are performed. The first is a 140-yr preindustrial control run (CONT) with all the climate forcings (e.g. aerosols and greenhouse gases) set at their 1860 (pre-industrial) levels. The perturbed case is a 100-yr run (AERO) starting from year 41 of CONT with identical forcings as CONT but for aerosols (mass concentration) set at present-day (1996–2000 average) levels. The equilibrium response is assessed based on the last 80 years of the runs. Further details of the model experiment design can be found in Ming and Ramaswamy (2009).

The analysis focuses on winter (December – February) based on monthly means and identifies the aerosol-driven changes by examine the difference between AERO and CONT. The statistical significance of the anomalies is estimated using the two-tailed Student's t-test. Anomalies at or above 90% or 95% significance level are indicated by black dots or colored shading. South China is defined as the region in 24˚–30˚N, 100˚–122˚E, and is represented by the red box in Figure 1b.

3 Results

3.1 Circulation Changes North of 30˚N

The spatial distribution of radiative flux perturbation at top of atmosphere (estimated as radiative flux differences between a present-day simulation and a preindustrial simulation using the same sea surface temperature) is highly heterogeneous and features larger values over the NH mid-latitude land and their downwind oceanic regions (Figure S11 published as Figure 1 of M11). The latitude-pressure cross-section of potential temperature changes, averaged over 60˚E–120˚W, is shown in Figure 1a. Aerosols cause cooling at all latitudes throughout the whole troposphere where atmospheric longwave irradiance dominates shortwave absorption by aerosols (Graf, 2004). Conversely, there is heating in the lower stratosphere except at the North Pole resulting from shortwave absorption by aerosols and ozone at stratosphere (Ferraro et al., 2011). The strongest warming appears at the South (summer) Pole; by contrast, the North (winter) Pole is under polar night condition and thus longwave cooling dominates. The tropospheric cooling is largest in the mid-latitudes of the NH where the aerosol loading is high. This too strong cooling near 60˚N is attributed to overestimated sulfate optical depth due to excessive hygroscopic growth in the model (Ginoux et al. 2006; Ocko et al., 2012). The cooling in the mid-latitudes strengthens the meridional temperature gradient between tropical and subtropical regions, while it weakens the gradient between the mid-latitudes and the polar region. Based on the thermal wind relation, the subtropical jet intensifies and shifts southward slightly, while the polar front jet weakens (Figure 1b and Figure S17), leading to a stronger EAWM circulation (Hu et al., 2015). To the northern flank of the subtropical jet, the East Asian trough remarkably deepens characterized by an elongated belt with negative 500-hPa geopotential height anomalies extending from central Asia to the central Pacific (Figure 1c). The mid-upper tropospheric circulation anomalies favor the occurrence of cold-air intrusions and thus, an intensified EAWM circulation (Zhang et al., 1997; Chen et al., 2014; Luo and Zhang, 2015).

3.2 Circulation Changes South of 30˚N

The tropical circulation response to aerosol forcing manifests in a southward shift of the Hadley circulation (Ming and Ramaswamy, 2011; Hwang et al., 2013) which induce an anomalous northward cross-equatorial energy transport to compensate for the interhemispheric energy imbalance due to stronger aerosol cooling in the NH. The vertical cross-section of the anomalous vertical velocity averaged over 60˚E–120˚W is shown in shading in Figure 2c. In the climatology (contours), the ascending branch of the regional Hadley cell is located within

10˚ north/south of the equator, with strongest upward motion at the equator. Under aerosols forcing, anomalous strong ascent (decent) appears around 10˚S (10˚N), indicating a southward shift of the Hadley cell. As a result, an anomalous meridional circulation also develops, featuring northward flow in the upper-troposphere and returning near-surface southward winds (e.g. Hwang et al., 2013; Wang et al., 2016). Not surprisingly, the pattern of anomalous vertical motion is associated with remarkable precipitation anomalies (Figure 4b) and, in particular, a southward shift of the ITCZ, consistently with the above studies. The spatial distribution of velocity potential χ and divergent circulation V_χ at 850 hPa and 200 hPa are shown in Figure 2a and Figure 2b, respectively. An upper-tropospheric strong large-scale divergence flow is observed from the SH to the NH within deep tropics, consistently with the anomalous ascent (descent) motion in the southern (northern) tropics. The divergent flow enhances the cross-hemispheric meridional dry static energy transport, counteracting the interhemispheric asymmetry in aerosol radiative cooling and smoothing the temperature gradient within the tropics (Chung and Soden, 2017; Hwang et al., 2013). This change in the large-scale atmospheric circulation in the upper troposphere, in turn, drives the low-level cross-equatorial wind in the opposite direction. A distinct low tropospheric divergence center south of the Philippines is in accord with the descending branch of the anomalous Hadley cell there. To the northwest of the divergent flow center, southwesterly anomalies prevail over China south of 30˚N, opposing the climatological EAWM flow.

3.3 Responses of EAWM

The aerosol-induced large-scale circulation changes discussed above are characterized by a southward movement of jet stream over the extratropics and of local Hadley cell over the tropics. Interannual changes in the above circulation features have shown an important and opposite imprint on monsoon circulation and precipitation amount over South China: a stronger EAWM and drier conditions associated with the southward shift of the jet, as opposed to a weaker EAWM and wetter conditions together with the Hadley cell southward migration (Wang and Chen, 2014; Zhang et al., 2014). The competition between tropical and extratropical circulation forcing on the EAWM is further investigated.

Figure 3a shows a clear dipole in the 850-hPa wind response over the northeastern Asia and the western Pacific, consisting of an anomalous cyclone over the Northwest Pacific with associated northerly anomalies, and an anomalous anticyclone to the southwest of the Philippines with associated southerly anomalies. The flow turns to westerlies at about 30˚N, which separates the two pressure anomalies. The northerly blows from the North China Plain to South China along the west edge of the anomalous cyclone centered near 30˚N, 180˚, suggesting a stronger EAWM. This anomalous cyclone is related to the southward shift of Aleutian low induced by the anomalous diabatic heating over the tropical East Pacific (see Figure 11 of M11). South of 30˚N, a strong anticyclone appears near 10˚N in accord with the low-level divergence flow (Figure 2b) and the descending motion of the local anomalous Hadley circulation (Figure 2c). Situated to the northwest of the anticyclone, the strong southwesterly flow suggests a weaker EAWM.

To provide further context to the dynamical dipole pattern discussed above, four indices representing the EAWM monsoon are computed. Two of them are defined for regions to the north of 30˚N, based on the zonal sea level pressure gradient and the meridional gradient of 300-hPa zonal wind (Chan and Li, 2004; Jhun and Lee, 2004). By contrast, the other two indices are defined for regions to the south of 30˚N, computed as areal-averaged meridional wind speed (Ji et al., 1997; Lu and Chan, 1999). More specific details on the definition of these indices are provided in Table S1, and the regions used to calculate areal average are displayed in Figure S12.

Note that, by choice, the former indices are more suitable to represent the extratropical variability of the EAWM, while the latter emphasizes the monsoon links with the tropics. Based on 80 years of data for each experiment, a Monte Carlo bootstrapping method (Efron and Tibshirani, 1993) is applied to estimate the probability density function (PDF) of the EAWM indices based on 40000 random samples drawn from the 80-year sequence, assuming independency between the data and equal probability of occurrence for any sequence of data, including repetitions. Figure 3b–e shows that aerosols tend to strengthen the monsoon circulation in the extratropics, while they weaken it in the tropics, consistently with the low-level circulation changes discussed above.

3.4 Responses of Precipitation over South China

It is conceivable that the remarkable circulation response pattern to aerosol forcing may result in precipitation anomalies via modulation of oceanic moisture transport toward the land in the tropics (Li et al., 2013). Figure 4a shows the spatial distribution of the 850-hPa anomalous moisture fluxes (MF; vector) and their convergence. The similarity with the anomalous 850-hPa wind pattern (Figure 3) is notable south of 30˚N, corroborating the link between circulation and precipitation anomalies. The prominent anticyclone over the south of the SCS is associated with anomalous moisture flux divergence. To the northwestern flank of the anticyclone, southwesterlies transport moisture to the eastern flank of the Indo-China Peninsula from the SCS and the Bay of Bengal. Further to the north, this flow splits into two branches: one branch flows into South China and extends to the Okhotsk Sea across Japan with associated moisture flux convergence (MFC; shading), the other turns eastward across the subtropical western Pacific where it results in an elongated belt of anomalous convergence in 10˚–20˚N, 120˚–180˚E. Notable cross-equatorial airflow blows from the NH to the SH, resulting in anomalous convergence (divergence) over the southern (northern) deep tropics. The circulation changes, in turn, result in southward shift of tropical rainfall belt (Figure 4b), consistently across different models (Williams et al., 2001; Fischer-Bruns et al., 2009; Chung and Soden, 2017). The pattern of precipitation (Figure 4b) within tropics bears a strong resemblance to that of MFC (Figure 4a) calculated based on monthly means, suggesting that the tropical precipitation is mainly driven by MFC on timescale longer than a month. By contrast, the discrepancy of patterns over extra-tropics indicates that the submonthly time scale processes (e.g., storm track) are of importance there. The precipitation is characterized by a zonally elongated positive anomaly stretching from the Indo-Gangetic Plain to the central extratropical Pacific, with a corresponding drying to the north, suggestive of a southward shift of the climatological precipitation. Ming et al. (2011) linked this anomalous pattern to variations in the southward movement of the North Pacific storm track.

This is further examined by analyzing the differences between precipitation minus evaporation (P – E) and the column-integrated MFC (Figure 4c). P – E and MFC should be balanced in climatology. However, note that the P – E includes atmospheric processes on all the timescales, while MFC is on timescales longer than a month as discussed above. Thus the (P – E) – MFC indicates the processes on submonthly scales, dominated by the storm track effects over extratropical regions. Noticeable zonal positive-negative alternating pattern appears over the sea while a much more scattered feature is seen over the land, indicating a stronger impact of storm track over the sea. The (P – E) – MFC over South China is negative in contradiction to precipitation increase there. Consequently, we conclude that the enhanced precipitation over South China is mainly attributed to the MFC increase induced by tropical circulation changes. The wetter conditions over South China also suggest a weaker EAWM (Wang and Chen, 2014).

4 Summary and Discussion

This study aims to investigate the effect of aerosols on the EAWM circulation and subsequent influence on regional precipitation during winter. Figure 5 schematically summarizes the mechanisms. Aerosol-induced changes in the EAWM can be understood by examining the circulation changes over tropical and extratropical regions separately (bordered by 30˚N). North of 30˚N, the aerosol-induced cooling in the midlatitudes leads to an intensified subtropical jet stream while the polar jet stream weakens. This pattern results in southward movement of the jet stream, a deepening of the East Asian trough, and a strengthening of northerly flow over the North China Plain, suggesting a stronger EAWM. By contrast, south of 30˚N, due to the interhemispheric asymmetric aerosol forcing, the local Hadley circulation shifts southward to compensate for the stronger aerosol cooling in the NH through cross-equatorial dry static energy flow (see Figure 6 of Ming and Ramaswamy, 2011). The circulation changes within deep tropics are characterized by anomalous subsidence over the NH while ascent over the SH. Corresponding to the anomalous subsidence around 10˚N, a prominent anticyclone is seen to the southwest of the Philippines. A pronounced southwesterly surface wind prevails over the SCS, indicating a weaker EAWM.

Enhanced MFC results in precipitation increase over South China. The distribution of (P – E) – MFC mainly subjects to the storm track in extratropical regions. The negative anomalies over South China in Figure 4c suggest that the enhanced precipitation over South China is results of the MFC increase driven by aerosol-induced tropical circulation (i.e., Hadley circulation) changes. This finding indicates the importance of Hadley circulation in regulating the intensity of EAWM and precipitation over South China. As the Hadley circulation change is attributed to aerosol-induced interhemispheric cooling, this hints that the effects of aerosols on EAWM above decadal timescale should be examined at a global scale.

Strong (weak) winter monsoon is always associated with significant surface cooling (warming). The aerosol-induced temperature changes are displayed in Figure 4d. Almost all values are negative, representing a cooling effect. A smaller temperature decrease over South China may indicate the anomalous warming due to weaker monsoon there. However, this secondary impact cannot offset the primary aerosol radiative cooling (Figure S9e). Note that the model uses a slab ocean model of uniform depth (50 m). While this precludes the full ocean response to aerosol, sea surface temperature (SST) is still allowed to respond to air-sea interactions (Figure 4). Moreover, the EAWM intensity is driven by processes generating over the continent (Ma et al., 2018), suggesting that the deep ocean response would play a secondary role in the overall aerosol impact.

One may wonder whether the aerosol-induced anomalies in precipitation and circulation found above are recognizable in observations, given the steady increase in Asian aerosol emissions since the 1950s up to the first decade of the 21st century (Figure S13). The EAWM intensity changes are examined by looking at PDF differences of the EAWM indices between 1980–2001 and 1958–1979 in the ERA40 dataset. The monsoon strengthens (weakens) north (south) of 30˚N during 1980–2001, as attested by larger (smaller) indices (Figure S14), consistently with the results discussed in Section 3.3. Figure S15 shows the precipitation changes between 1986–2000 and 1960–1974 in the CRU dataset, with a distinct increase over South China. In addition, based on daily meteorological observations in China, the 1955–2010 linear trend also shows a salient pattern of increase over South China, further confirming the precipitation increases there (Figure S16). These findings may support the argument that the importance of aerosol-induced changes in EAWM and associated precipitation over South China. And the impact on circulation can differ across different latitudes. In addition to the changes in the intensity of the EAWM, the interannual variability

of the EAWM may also change with aerosol forcing. An inspection on the standard deviation of the EAWM index (Figure S18) suggests that the interannual variability of the EAWM generally becomes stronger with enhanced aerosol forcing, implying that more extreme EAWM years are likely to occur in responses to increased aerosols.

We acknowledge that there are some uncertainties in the model representation of aerosol effects. The aerosol radiative forcing is –1.72 W m^{-2} (Figure S9a), which is larger than the CMIP5 ensemble mean (–1.17 W m^{-2}; Zelinka et al., 2014). Note the slab ocean is used rather than fixed SST which is commonly used for aerosol forcing estimation. The stronger aerosol forcing means that the results are likely to represent an upper bound of the aerosol impact. The aerosol optical depth is overestimated in the NH (particularly at midlatitude) while underestimated in the SH (Figure S3). On the one hand, the excessive cooling bias at midlatitude exacerbates (weakens) the meridional temperature gradient equatorward (poleward) of the subtropical jet. As a consequence, the further southward shift of jet is induced. On the other hand, the larger interhemispheric energy imbalance generates a stronger southward shift of local Hadley cell. The overall changes in EAWM strength and associated precipitation depend on the competing effects of southward shift of the jet stream and of the local Hadley cell. The robustness of the findings needs to be evaluated by analyzing the output from other climate models. Nevertheless, the results provide evidence on the influence of aerosols on EAWM and precipitation over South China with competing tropical and extratropical mechanisms. This important topic has been mainly overlooked so far.

Acknowledgments, Samples, and Data

We thank the two anonymous reviewers whose insightful comments lead to a significant improvement of the manuscript. This work is jointly supported by the Early Career Scheme of Research Grants Council of Hong Kong (grant CUHK24301415), the National Key Basic Research Program of China (grant 2015CB954103), the Improvement on Competitiveness in Hiring New Faculties Fund (2013/2014) of The Chinese University of Hong Kong (grant 4930059), and the Vice-Chancellor's Discretionary Fund of The Chinese University of Hong Kong (grant 4930744). The appointment of NCL at CUHK is supported by the AXA Research Fund. We would also like to acknowledge Met Office Climate Science for Service Partnership China as part of the Newton Fund for supporting Zhen Liu and Massimo A. Bollasina on the paper revision effort. Ming Luo is supported by the National Natural Science Foundation of China (grant 41871029). Lin Wang is supported by the Chinese Academy of Sciences (grant QYZDY-SSW-DQC024). Zhen Liu acknowledges the Global Scholarship Program for Research Excellence 2017-18 at The Chinese University of Hong Kong to support his exchange visit to Princeton University. The model simulations are conducted on the Gaia computer at NOAA GFDL and the results are archived at GFDL. The GPCP datasets for precipitation are available from the website https://www.esrl.noaa.gov/psd/data/gridded/data.gpcp.html. The JRA-55 reanalysis product for wind is provided by the Japan Meteorological Agency (https://rda.ucar.edu/datasets/ds628.1/).

References

Bollasina, M. A., Ming, Y., Ramaswamy, V., Schwarzkopf, M. D., & Naik, V. (2014). Contribution of local and remote anthropogenic aerosols to the twentieth century weakening of the South Asian monsoon. *Geophysical Research Letters*, *41*(2), 680–687. https://doi.org/10.1002/2013GL058183

Bollasina, M. A., Ming, Y., & Ramaswamy, V. (2011). Anthropogenic aerosols and the weakening of the South Asian summer monsoon. *Science*, *334*(6055).

Chan, J. C. L., & C. Y. Li (2004). The East Asia winter monsoon. *East Asian Monsoon*, pp. 54–106, C. P. Chang, Ed., World Scientific Publishing Co. Pet. Ltd., Singapore.

Chang, C.-P., Lu M.-M., and Wang B., 2011: The East Asian winter monsoon. *The Global Monsoon System: Research and Forecast*, Chang C.-P. et al., Eds., World Scientific Series on Asia-Pacific Weather and Climate, Vol. 5, World Scientific, 99–109.

Chang, C.-P., Wang Z., & H. Hendon (2006) The Asian winter monsoon. *The Asian Monsoon*, B. Wang, Ed., Springer, 89– 127.

Chen, W., Graf, H.-F., & Huang, R. (2000). The interannual variability of East Asian winter monsoon and its relation to the summer monsoon. *Advances in Atmospheric Sciences*, *17*(1), 48–60. https://doi.org/10.1007/s00376-000-0042-5

Chen, Z., Wu, R., & Chen, W. (2014). Distinguishing interannual variations of the northern and southern modes of the East Asian winter monsoon. *Journal of Climate*, *27*(2), 835–851. https://doi.org/10.1175/JCLI-D-13-00314.1

Chung, E. S., & Soden, B. J. (2017). Hemispheric climate shifts driven by anthropogenic aerosol-cloud interactions. *Nature Geoscience*, *10*(8), 566–571. https://doi.org/10.1038/NGEO2988

Das, S., Dey, S., & Dash, S. K. (2014). Impacts of aerosols on dynamics of Indian summer monsoon using a regional climate model. *Climate Dynamics*, 1685–1697. https://doi.org/10.1007/s00382-014-2284-4

Ding, Y. H. (1994). Monsoons over China, 432pp, Kluwer Academic Publishers.

Efron, B., & Tibshirani, R. J. (1993). An introduction to the bootstrap. Monographs on Statistics and Applied Probability, No. 57. *Chapman and Hall, London, 436 p*. https://doi.org/10.1111/1467-9639.00050

Ferraro, A. J., Highwood, E. J., & Charlton-Perez, A. J. (2011). Stratospheric heating by potential geoengineering aerosols. *Geophysical Research Letters*, *38*, L24706. https://doi.org/10.1029/2011GL049761

Fischer-Bruns, I., Banse, D. F., & Feichter, J. (2009). Future impact of anthropogenic sulfate aerosol on North Atlantic climate. *Climate Dynamics*, *32*(4), 511–524. https://doi.org/10.1007/s00382-008-0458-7

GFDL Global Atmospheric Model Development Team (2004). The new GFDL global atmosphere and land model AM2LM2: Evaluation with prescribed SST simulations. *Journal of Climate*, *17*(24), 4641–4673, doi:10.1175/JCLI-3223.1.

Graf, H. F. (2004). The complex interaction of aerosols and clouds. *Science*. https://doi.org/10.1126/science.1094411

Guo, L., Highwood, E. J., Shaffrey, L. C., & Turner, A. G. (2013). The effect of regional changes in anthropogenic aerosols on rainfall of the East Asian Summer Monsoon. *Atmospheric Chemistry and Physics*, *13*(3), 1521–1534. https://doi.org/10.5194/acp-13-1521-2013

Horowitz, L. W. (2006). Past, present and future concentrations of tropospheric ozone and aerosols: Methodology, ozone evaluation, and sensitivity to aerosol wet removal. *Journal of Geophysical Research Atmospheres*, *111*(22). https://doi.org/10.1029/2005JD006937

Hu, C., Yang, S., & Wu, Q. (2015). An optimal index for measuring the effect of East Asian winter monsoon on China winter temperature. *Climate Dynamics*, *45*(9–10), 2571–2589. https://doi.org/10.1007/s00382-015-2493-5

Huang, J., Wang, T., Wang, W., Li, Z., & Yan, H. (2014). Climate Effects of dust aerosols over east asian and semiarid regions. *Journal of Geophysical Research: Atmospheres*, 1–19. https://doi.org/10.1002/2014JD021796.

Hwang, Y. T., Frierson, D. M. W., & Kang, S. M. (2013). Anthropogenic sulfate aerosol and the southward shift of tropical precipitation in the late 20th century. *Geophysical Research Letters*, *40*(11), 2845–2850. https://doi.org/10.1002/grl.50502

Jhun, J.-G., & Lee, E.-J. (2004). A new East Asian winter monsoon index and associated characteristics of the winter monsoon. *Journal of Climate*, *17*(4), 711–726. https://doi.org/10.1175/1520-0442(2004)017<0711:ANEAWM>2.0.CO;2

Ji, L., Sun, S., Arpe, K., & Bengtsson, L. (1997). Model study on the interannual variability of Asian winter monsoon and its influence. *Advances in Atmospheric Sciences*, *14*(1), 1–22. https://doi.org/10.1007/s00376-997-0039-4

Jiang, Y., Yang, X. Q., Liu, X., Yang, D., Sun, X., Wang, M., … Fu, C. (2017). Anthropogenic aerosol effects on east asian winter monsoon: The role of black carbon-induced tibetan plateau warming. *Journal of*

Geophysical Research, *122*(11), 5883–5902. https://doi.org/10.1002/2016JD026237
Kim, M. J., Yeh, S.-W., & Park, R. J. (2016). Effects of sulfate aerosol forcing on East Asian summer monsoon for 1985-2010. *Geophysical Research Letters*, *43*(3), 1364–1372. https://doi.org/10.1002/2015GL067124
Kim, M. J., Yeh, S.-W., Park, R. J., Son, S.-W., Moon, B.-K., Kim, B.-G., … Kim, S.-W. (2019). Regional Arctic amplification by a fast atmospheric response to anthropogenic sulphate aerosol forcing in China. *Journal of Climate*. https://doi.org/10.1175/jcli-d-18-0200.1
Koren, I., Dagan, G., & Altaratz, O. (2014). From aerosol-limited to invigoration of warm convective clouds. *Science*, *344*(6188), 1143–1146. https://doi.org/10.1126/science.1252595
Lau, K.M., & Chang C.-P. (1987). Planetary scale aspects of winter monsoon and teleconnections. *Monsoon Meteorology*, 161-202. Chang C.-P. and Krishnamurti, Eds., Oxford University Press.
Lau, K.-M., Tsay, S. C., Hsu, C., Chin, M., Ramanathan, V., Wu, G.-X., … Zhang, R. (2008). The joint aerosol–monsoon experiment: A new challenge for monsoon climate research. *Bulletin of the American Meteorological Society*, *89*(3), 369–383. https://doi.org/10.1175/BAMS-89-3-369
Lau, K. M., Kim, M. K., & Kim, K. M. (2006). Asian summer monsoon anomalies induced by aerosol direct forcing: The role of the Tibetan Plateau. *Climate Dynamics*, *26*(7–8), 855–864. https://doi.org/10.1007/s00382-006-0114-z
Li, X.Z., Zhou W., Li C.Y., & Song J. (2013). Comparison of the annual cycles of moisture supply over southwest and southeast China. *Journal of Climate*, 26:10139–10158
Li, Z., Li, C., Chen, H., Tsay, S. C., Holben, B., Huang, J., … Zhuang, G. (2011). East Asian Studies of Tropospheric Aerosols and their Impact on Regional Climate (EAST-AIRC): An overview. *Journal of Geophysical Research Atmospheres*, *116*(4). https://doi.org/10.1029/2010JD015257
Liu, G., Ji, L.-R., Sun, S.-Q., & Xin, Y.-F. (2012). Low- and mid-high latitude components of the East Asian winter monsoon and their reflecting variations in winter climate over Eastern China. *Atmospheric and Oceanic Science Letters*, *5*(3), 195–200. https://doi.org/10.1080/16742834.2012.11446985
Liu, G., Ji, L., Sun, S., & Xin, Y. (2013). A discussion on the East Asian winter monsoon index—Differences between the East Asian winter monsoon at mid-high and low latitudes (in Chinese). *Chinese Journal of Atmospheric Sciences*, *37*(3), 755–764. https://doi.org/doi:10.3878/j.issn. 1006-9895.2012.12054.
Lu, E., & Chan, J. C. L. (1999). A unified monsoon index for south China. *Journal of Climate*, *12*(8 PART 1), 2375–2385. https://doi.org/10.1175/1520-0442(1999)012<2375:AUMIFS>2.0.CO;2
Luo, X., & Zhang, Y. (2015). The linkage between upper-level jet streams over East Asia and East Asian Winter Monsoon variability. *Journal of Climate*, *28*(22), 9013–9028. https://doi.org/10.1175/JCLI-D-15-0160.1
Ma, T., Chen, W., Feng, J., & Wu, R. (2018). Modulation effects of the East Asian winter monsoon on El Niño-related rainfall anomalies in southeastern China. Scientific Reports. https://doi.org/10.1038/s41598-018-32492-1
Ming, Y., Ramaswamy, V., & Chen, G. (2011). A model investigation of aerosol-induced changes in boreal winter extratropical circulation. *Journal of Climate*, *24*(23), 6077–6091. https://doi.org/10.1175/2011JCLI4111.1
Ming, Y., Ramaswamy, V., Donner, L. J., Phillips, V. T. J., Klein, S. a., Ginoux, P. a., & Horowitz, L. W. (2007). Modeling the interactions between aerosols and liquid water clouds with a self-consistent cloud scheme in a general circulation model. *Journal of the Atmospheric Sciences*, *64*(4), 1189–1209. https://doi.org/10.1175/JAS3874.1
Ming, Y., & Ramaswamy, V. (2009). Nonlinear climate and hydrological responses to aerosol effects. *Journal of Climate*, *22*(6), 1329–1339. https://doi.org/10.1175/2008JCLI2362.1
Ming, Y., & Ramaswamy, V. (2011). A model investigation of aerosol-induced changes in tropical circulation. *Journal of Climate*, *24*(19), 5125–5133. https://doi.org/10.1175/2011JCLI4108.1
Nakajima, T., Yoon, S. C., Ramanathan, V., Shi, G. Y., Takemura, T., Higurashi, A., … Schutgens, N. (2007). Overview of the atmospheric brown cloud East Asian regional experiment 2005 and a study of the aerosol direct radiative forcing in East Asia. *Journal of Geophysical Research Atmospheres*. https://doi.org/10.1029/2007JD009009
Ramanathan, V., Crutzen, P. J., Lelieveld, J., Mitra, A. P., Althausen, D., Anderson, J., … Valero, F. P. J. (2001). Indian Ocean Experiment: An integrated analysis of the climate forcing and effects of the great Indo-Asian haze. *Journal of Geophysical Research: Atmospheres*, *106*(D22), 28371–28398. https://doi.org/10.1029/2001JD900133
Wang, B., Wu, Z., Chang, C. P., Liu, J., Li, J., & Zhou, T. (2010). Another look at interannual-to-interdecadal variations of the East Asian winter monsoon: The northern and southern temperature modes. *Journal of Climate*, *23*(6), 1495–1512. https://doi.org/10.1175/2009JCLI3243.1
Wang, L., & Chen, W. (2014). An intensity index for the East Asian winter monsoon. *Journal of Climate*, *27*(6), 2361–2374. https://doi.org/10.1175/JCLI-D-13-00086.1
Wang, L., & Lu, M.-M. (2017) The East Asian winter monsoon. *The Global Monsoon System: Research and Forecast* (3rd Edition).Edited by C.-P. Chang, H.-C. Kuo, N.-C. Lau, R. H. Johnson, B. Wang, and M.

Wheeler, 51-61, doi: 10.1142/9789813200913_0005
Wang, H., Xie, S. P., & Liu, Q. (2016). Comparison of climate response to anthropogenic aerosol versus greenhouse gas forcing: Distinct patterns. Journal of Climate. https://doi.org/10.1175/JCLI-D-16-0106.1
Williams, K. D., Jones, A., Roberts, D. L., Senior, C. A., & Woodage, M. J. (2001). The response of the climate system to the indirect effetcs of anthropogenic sulfate aerosol. *Climate Dynamics*, *17*(11), 845–856. https://doi.org/10.1007/s003820100150
Yeh, S. W., Park, R. J., Kim, M. J., Jeong, J. I., & Song, C. K. (2015). Effect of anthropogenic sulphate aerosol in China on the drought in the western-to-central US. *Scientific Reports*. https://doi.org/10.1038/srep14305
Yeh, S. W., So, J., Lee, J. W., Kim, M. J., Jeong, J. I., & Park, R. J. (2017). Contributions of Asian pollution and SST forcings on precipitation change in the North Pacific. *Atmospheric Research*. https://doi.org/10.1016/j.atmosres.2017.03.014
Zhang, L., Fraedrich, K., Zhu, X., Sielmann, F., & Zhi, X. (2014). Interannual variability of winter precipitation in Southeast China. *Theoretical and Applied Climatology*, *119*(1–2), 229–238. https://doi.org/10.1007/s00704-014-1111-5
Zhang, Y., Sperber, K. R., & Boyle, J. S. (1997). Climatology and interannual variation of the East Asian winter monsoon: results from the 1979–95 NCEP/NCAR reanalysis. *Monthly Weather Review*, *125*(10), 2605–2619. https://doi.org/10.1175/1520-0493(1997)125<2605:CAIVOT>2.0.CO;2

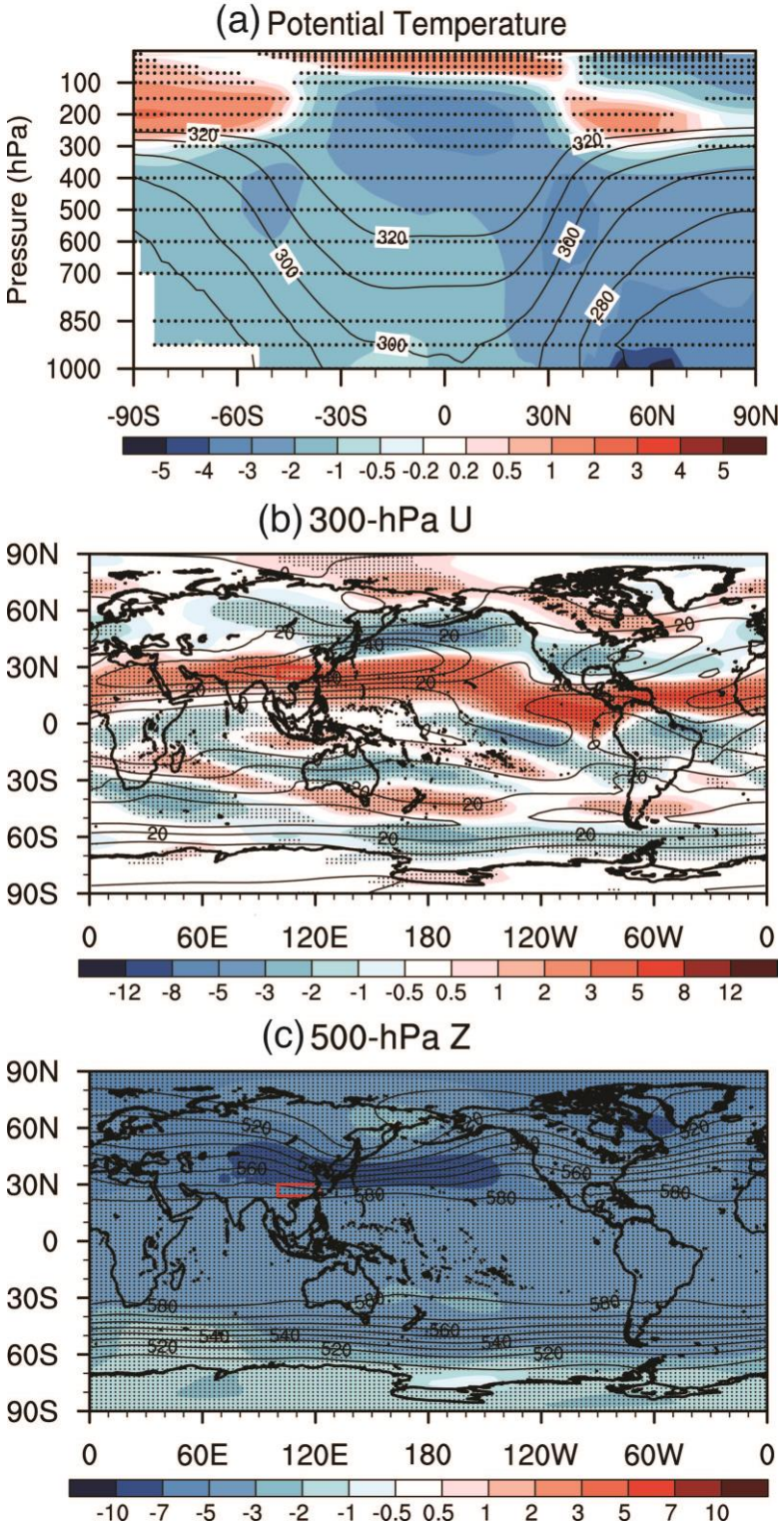

Figure 1. Effects of increased aerosol measured as the differences between AERO and CONT (shading). (a) latitude-pressure cross-section of potential temperature (K) averaged over 60˚E – 120˚W, (b) 300-hPa zonal wind (m s^{-1}), and (c) 500-hPa height (10 m). The climatology in CONT is indicated by the contour lines. Black dots denote differences at the 95% significance level according to the two-tailed Student's t-test. The red boxes denote South China.

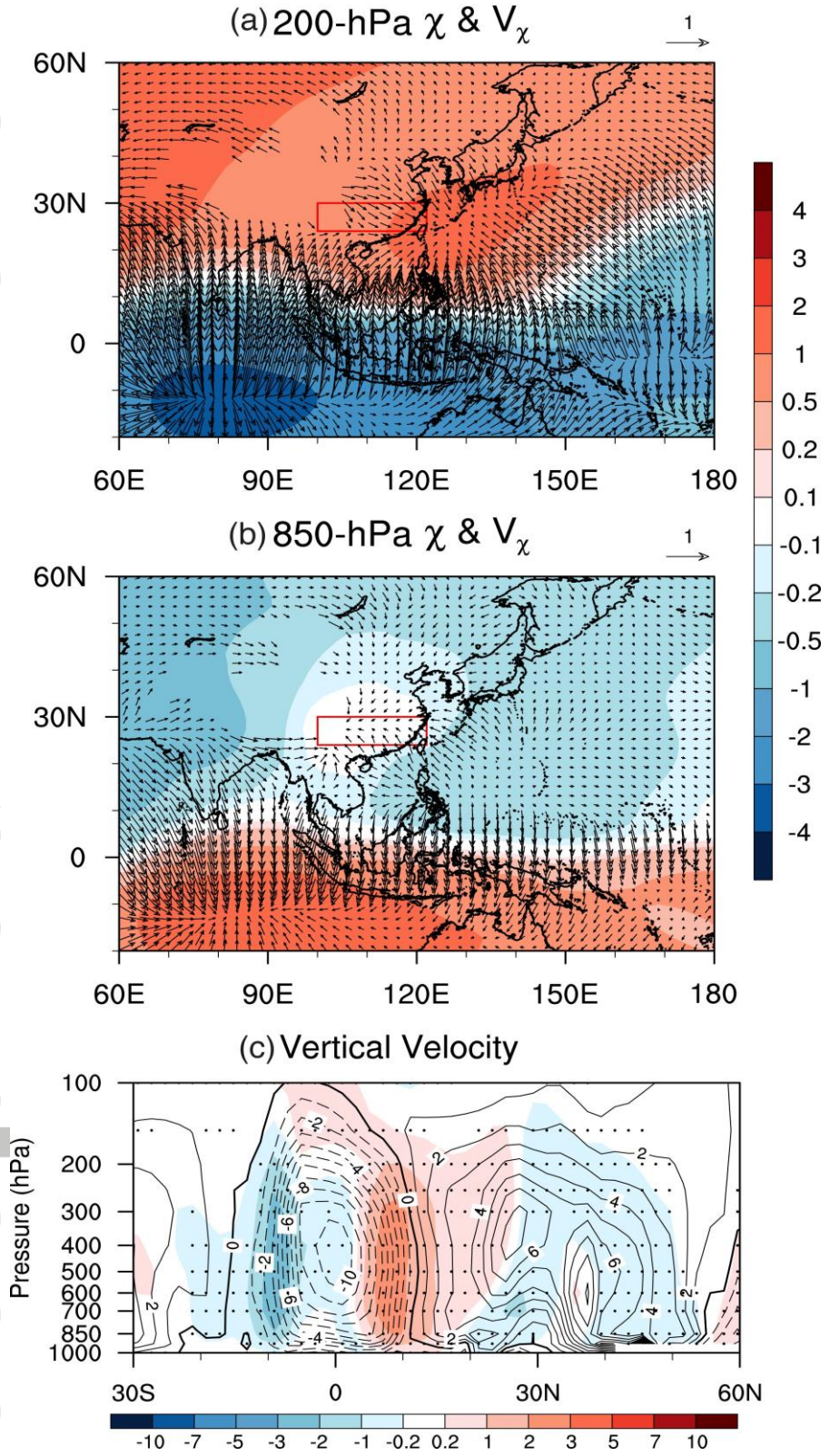

Figure 2. Effects of increased aerosol measured as the differences between AERO and CONT. (a) 200-hPa and (b) 850-hPa velocity potential (shading; 10^6 m^2 s^{-1}) and divergent wind (vector; m s^{-1}), and (c) latitude-pressure cross-section of vertical velocity (shading; 0.01 Pa s^{-1}) averaged over 100˚E – 122˚E). Red (blue) indicate descent (ascent). The climatology in CONT is indicated by the contour lines in (c). Solid (dashed) contours denote descent (ascent), and the bold solid line marks the zero contour.

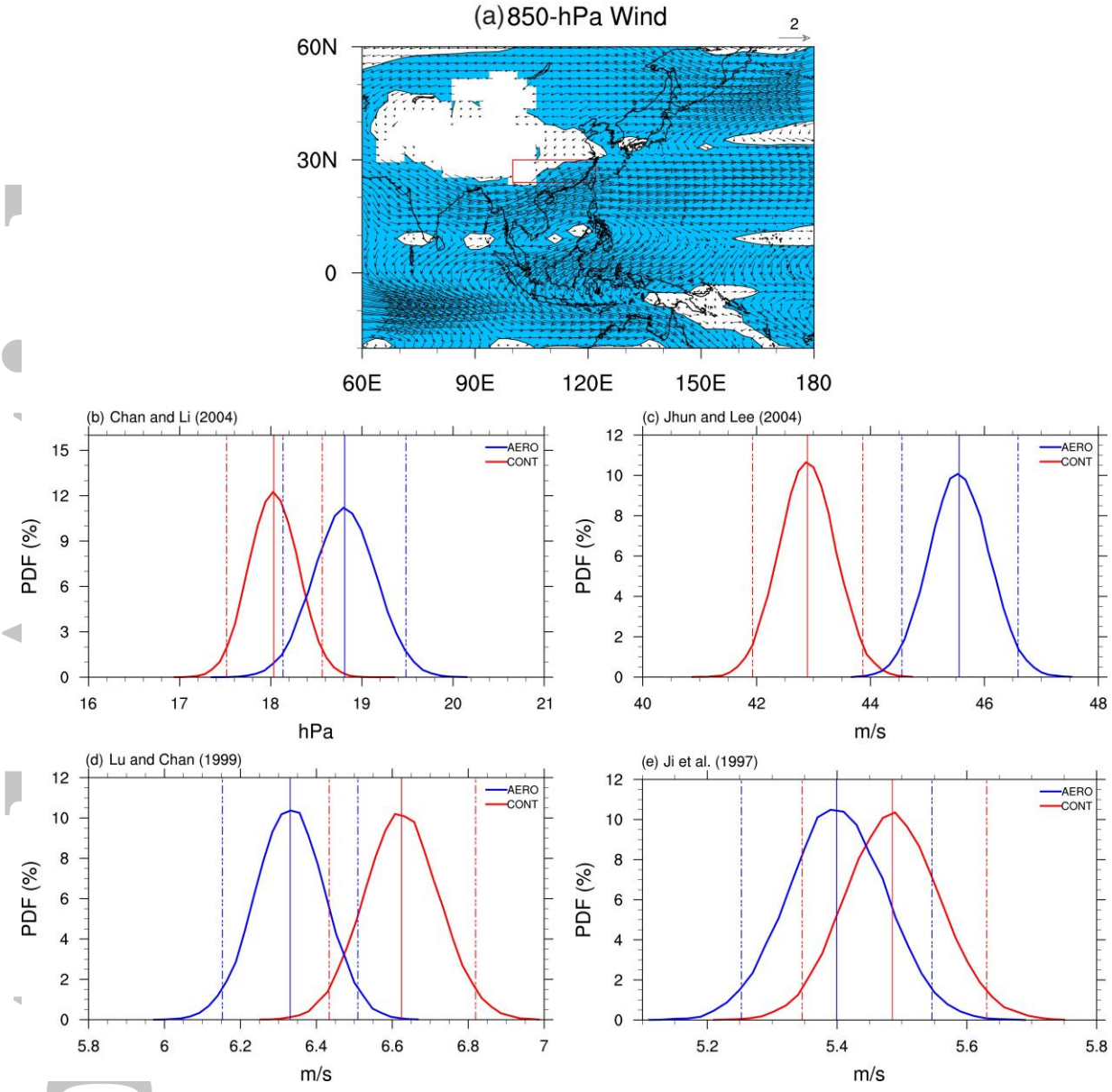

Figure 3. (a) Effect of increased aerosols on 850-hPa wind (vector; m s^{-1}) measured as the differences between AERO and CONT. Blue shading indicates the wind differences at the 95% significance level. Probability distribution function (PDF; curve) and median (vertical solid line) of the annual East Asian winter monsoon index defined in (b) Chan and Li (2004), (c) Jhun and Lee (2004), (d) Lu and Chan (1999), and (e) Ji et al. (1997) in the CONT (red) and the AERO (blue). The vertical dash lines denote the 5% and 95% percentiles, respectively. The definitions of four East Asian winter monsoon indices are listed in Table S1. Corresponding boundaries for computing the areal averages are denoted by rectangles in Figure S12.

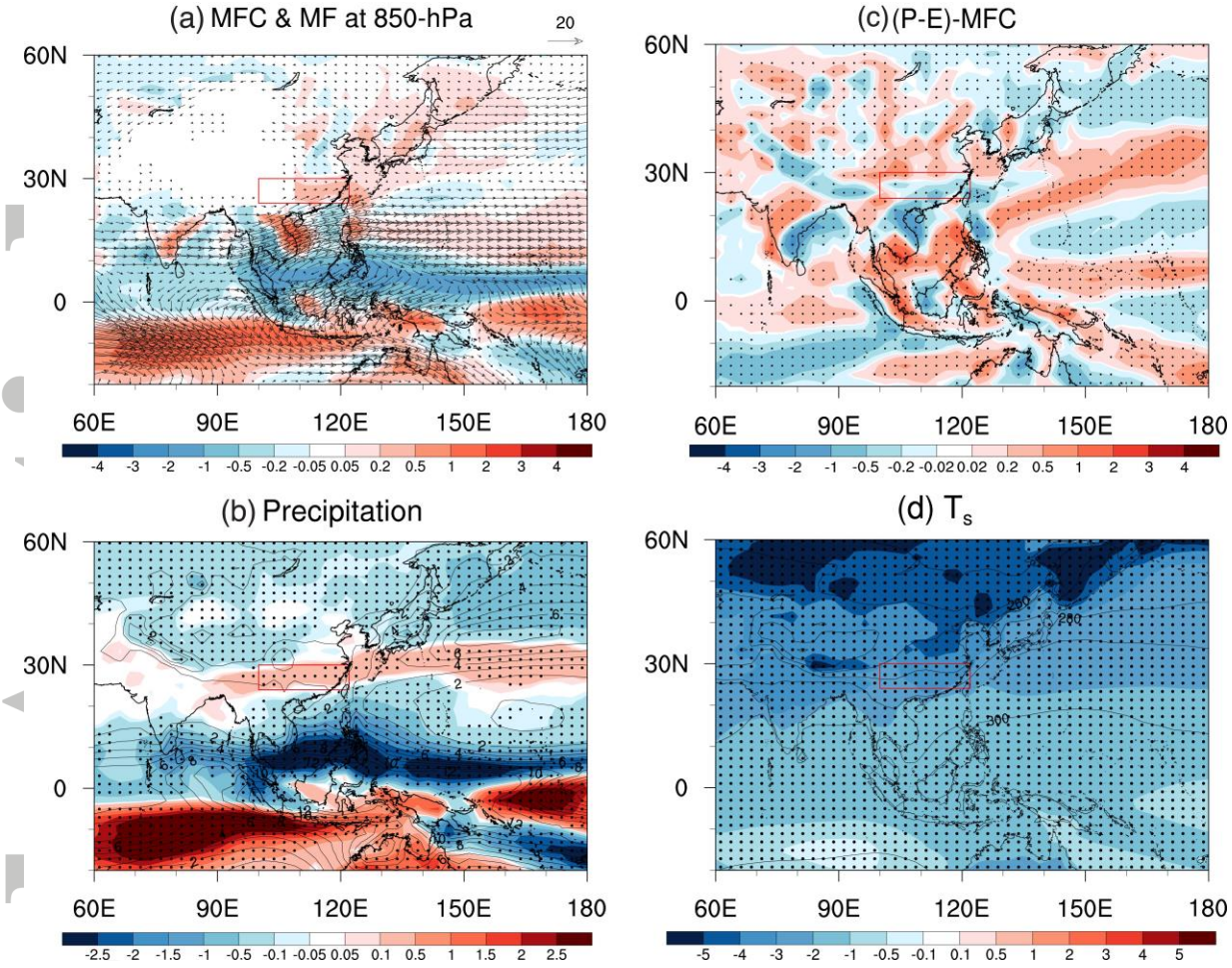

Figure 4. Effects of increased aerosol measured as the differences between AERO and CONT. (a) moisture flux convergence (MFC; shading; 10^{-5} g kg^{-1} s^{-1}) and moisture flux (MF; vector; g kg^{-1} m s^{-1}) at 850-hPa, (b) precipitation (shading; mm day^{-1}), (c) precipitation minus evaporation (P – E) minus column-integrated MFC (shading, mm day^{-1}), and (d) surface temperature (shading; K). Red (blue) shading denotes convergence (divergence) in (a). The climatology in CONT is indicated by the contour lines in (b) and (d). Black dots denote differences at the 90% significance level in (b) and (c) and 95% significance in (d).

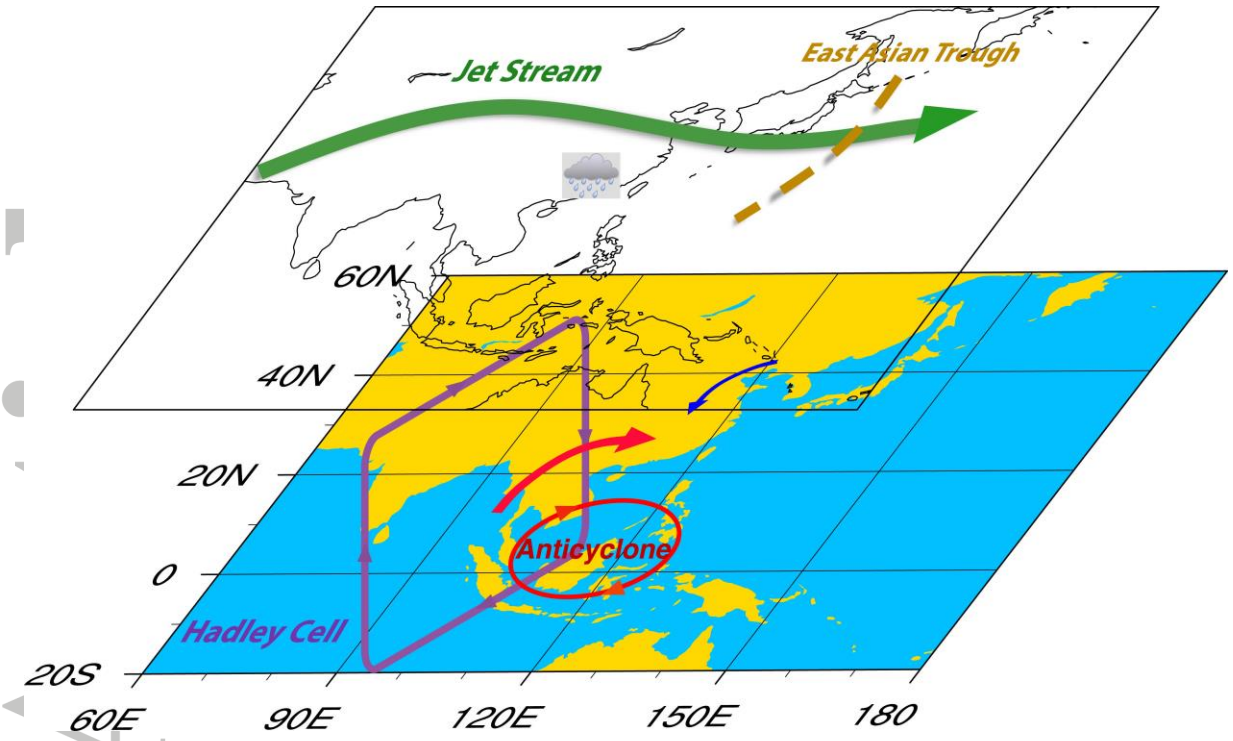

Figure 5. Schematic diagram showing the mechanism of aerosol-induced changes in the East Asian winter monsoon and precipitation over South China.